

Laser-Induced Breakdown Spectroscopy for the Analysis of Cobalt–Chromium Orthopaedic Wear Debris Particles

E. A. MOKHBAT and D. W. HAHN*

Department of Mechanical Engineering, University of Florida, Gainesville, Florida 32611

Laser-induced breakdown spectroscopy (LIBS) is investigated for the quantitative analysis of individual cobalt–chromium wear particles generated *in vivo* from human artificial knee joints. As implemented, the LIBS technique provided a measurement of the absolute chromium and cobalt masses for individual wear particles, which enabled calculation of chromium-to-cobalt mass ratios and the equivalent spherical diameter on a particle-to-particle basis. Using a multiple analyte emission line spectral filtering process, absolute cobalt and chromium mass measurements were made as low as 40 and 20 fg, respectively, corresponding to a particle diameter of approximately 200 nm. The size of the wear debris ranged from approximately 200 to 800 nm, with a mean diameter of 385 nm. In addition, the wear particles exhibited a depletion of cobalt with respect to the bulk composition of the cobalt–chromium alloy. The cobalt depletion exhibited a strong correlation with size, with the larger particles characterized by a more significant depletion of cobalt. All synovial fluid samples were inactivated with 10% bleach to reduce risks of infection by bloodborne pathogens. Control wear debris was generated from manual abrasion of pristine cobalt–chromium alloy specimens and analyzed with the LIBS technique to address the potential effects of bleach addition. No statistical differences were recorded between the particle suspensions treated and untreated with bleach. Overall, the LIBS method was successfully implemented for the quantitative analysis of cobalt–chromium wear particles.

Index Headings: LIBS; Laser-induced breakdown spectroscopy; Wear particles.

INTRODUCTION

Wear particles generated at the articulating surfaces of orthopaedic implants, namely total hip and knee prosthesis, continue to be of interest due to a general consensus among researchers regarding their association with periprosthetic osteolysis and aseptic loosening of joint systems, often resulting in premature implant failure. Particulate wear debris may include a wide range of particle types, including metallic particles and ultrahigh molecular weight polyethylene particles from the load bearing surfaces, as well as bone cement (polymethylmethacrylate or PMMA) or metal particles from the fixation surfaces. In commonly used metal on polyethylene implant systems, polyethylene wear rates greatly exceed the wear rates of the harder, counter bearing metal surfaces; hence, wear debris is dominated by polyethylene particles. While considerable resources have been focused on the role of wear debris in the many complex biological reactions involving foreign body particulates, there are parallel efforts underway to reduce overall wear debris levels using alternative implant systems that make use of metal-on-metal articulations.^{1–3} While metal-on-metal im-

plant systems are characterized by significant reductions in wear rates as compared to the popular metal-on-polyethylene systems, researchers must now consider more thoroughly the characteristics of metallic wear particles and the potential adverse effects on periprosthetic tissues, including toxicity, inflammation, and osteolysis, and ultimately on prosthesis loosening.

The significance of the type of small particles on the biological response has been studied in a variety of clinical and laboratory systems, including histology studies of tissue from implant retrievals, animal models, and cell culture studies. A number of studies have demonstrated a dependence of histiologic response on both the particle size and composition of particles tested.^{4–6} With regard to particle size, small particles (less than about 2 μm) will in general lead to a mononuclear histiocytic response, while larger particles will become engulfed by local phagocytic cells, isolating them from surrounding tissues. Phagocytosis, however, is often the initiation of more complex inflammatory responses that may culminate in tissue necrosis or bone resorption. With regard to particle type, recent studies have concluded that for biologically relevant particles sizes (i.e., submicrometer to $\sim 10 \mu\text{m}$), the chemical makeup of the particles is more important than the particle size. Of note, cobalt–chromium particles have been reported to be among the more biologically toxic particles as compared to polyethylene, PMMA, and aluminum–titanium–vanadium particles.^{7,8} Cobalt–chromium is the primary load-bearing alloy utilized in current metal-on-metal implant systems as well as with traditional metal-on-polyethylene prosthesis. Given the current interests in wear debris, as well as the increasing clinical use of new implant system designs, a need exists for relevant data concerning the characteristics (namely size and composition) of metallic wear particles.

To date, the most prevalent techniques as applied to the analysis of orthopaedic wear debris are visible light microscopy, scanning electron microscopy, and transmission electron microscopy. Visible light microscopy is useful for the identification of polyethylene wear debris due to polyethylene's pronounced birefringent nature, although larger metallic particles are also readily analyzed. Light microscopy, however, has several limitations regarding wear debris analysis, namely a resolution limit on the order of the wavelength of light, and the inability to type (i.e., identify composition) wear particles other than through visible observation, notwithstanding birefringence measurements. Metallic wear particles isolated from both periprosthetic tissue and synovial fluid samples are reported to range in size from as small as 10 nm to 50 μm , with the majority generally submicrometer sized,

Received 11 January 2002; accepted 15 March 2002.

* Author to whom correspondence should be sent.

as measured using various microscopy techniques;^{9–11} hence, light microscopy analysis will miss many of the smaller particles. Electron microscopy is well suited to analyze even the smallest metallic wear particles; however, sample preparation often leads to particle agglomeration, and therefore, care must be exercised when reporting size distributions. An added advantage of electron microscopy is the ability for concomitant composition measurements using energy dispersive X-ray (EDX) analysis. However, while electron microscopy offers the ability for the size and composition analysis of individual wear particulates, such measurements are laborious, and true quantitative measurements of constituent elemental concentrations are difficult due to limitations of uniform particle assay with EDX. In addition to the microscopy techniques outlined above, other analytical techniques include the use of atomic emission spectroscopy, including graphite furnace and inductively coupled plasma, for total metals analysis, and Raman spectroscopy for the analysis of individual particles. The focus of this paper is on the quantitative analysis of individual orthopaedic wear particles using a recently developed single-particle measurement scheme based on laser-induced breakdown spectroscopy (LIBS).

Laser-induced breakdown spectroscopy is an atomic emission spectroscopy technique like inductively-coupled plasma (ICP) spectroscopy; however, LIBS differs in that the plasma is created by a tightly focused, high power, pulsed laser beam. Research and review papers focusing on LIBS, including the study of chromium, lead, cadmium, calcium, potassium, magnesium, and zinc, are reported in the literature.^{12–16} The quantitative analysis of individual particles using the LIBS technique was recently demonstrated for laboratory analysis and analysis of ambient air particulate matter, including individual chromium, magnesium, and aluminum-based particles approaching sizes as small as 100 nm and elemental mass as low as 2 fg.^{17,18} The goal of this paper is to examine the feasibility and applicability of LIBS-based quantitative analysis of individual orthopaedic wear particles as obtained from synovial fluid suspensions.

EXPERIMENTAL METHODS

Laser-Induced Breakdown Spectroscopy Measurements. A brief overview of the LIBS experimental setup is presented here, with additional details reported previously.^{17,19} A schematic of the LIBS system is shown in Fig. 1. The excitation source was a 1064-nm Q-switched Nd:YAG laser with a nominal pulse width of 10 ns, maximum pulse energy of 350 mJ, and operated with a 5 Hz pulse repetition rate. The expanded laser beam (12-mm diameter) was focused into the sample chamber (2.75-in., stainless-steel 6-way vacuum cross) using a 75-mm UV grade lens to create the plasma ($f/6.25$). The plasma emission was collected along the incident beam in a backward direction and separated using a pierced mirror. The collected plasma emission was fiber-coupled to a 0.275-m spectrometer, dispersed with a 2400-groove/mm grating (0.03 nm/pixel, 0.12-nm resolution), and recorded with an intensified, charge-coupled device (iCCD) detector array. Aerosol streams were generated by nebulizing aqueous analyte solutions (deionized water with dis-

solved cobalt and chromium) into a gaseous co-flow stream of either dry nitrogen or purified, dry air. The nebulizer was a standard pneumatic nebulizer (Hudson model 1724) typically used for the dispersion of respiratory medications. Air was collected and compressed from the air-conditioned laboratory building, and then passed through a water separator, particle filter, pressure regulator, desiccant drier, and final HEPA filter prior to entering the flow controllers and sample chamber. Nitrogen was industrial grade, compressed dry nitrogen, and was regulated and passed through a HEPA filter and flow controller prior to use. All gas flows were controlled using electronic mass flow controllers.

Standard solutions (SPEX, Inc.) of dissolved metals were used for all calibration experiments. Calibration curves were generated using serial dilution of 10 000 $\mu\text{g}/\text{mL}$ of chromium in 5% HNO_3 , and 10 000 $\mu\text{g}/\text{mL}$ of cobalt in 5% HNO_3 . All dilution was performed using ultra-purified deionized water.

Inductively-Coupled Plasma Mass Spectrometry Measurements. ICP-MS measurements were performed using a Finnigan MAT SOLA ICP-MS system with a quadrupole mass analyzer and a radio frequency (Rf) power of 1200 W. The nebulizer solution uptake rate was 1 mL/min for all experiments.

Sample Collection and Processing. Synovial fluid samples used in this study were provided by the department of Orthopaedics and Rehabilitation at the University of Florida Health Science Center. The samples were collected from patients undergoing primary and revision total knee arthroplasty surgery. All patients gave formal consent, in accordance with an approved Institutional Review Board (IRB) protocol. The synovial fluid samples were processed in the orthopaedic research laboratory in accordance with all the Environmental Health and Safety policies on biological fluids and bloodborne pathogens. A summary of the sample processing follows. All samples were first inactivated using a dilution of 10% by volume of bleach (9 parts synovial fluid sample to 1 part bleach, namely 5.25% sodium hypochlorite) for a period no less than an hour. This was done in order to reduce the biohazard risks, thereby facilitating the handling of the samples during analysis, and minimizing the exposure of persons involved in handling the samples. Particular biohazards of concern were Hepatitis C and HIV. Samples were screened in advance for these pathogens and excluded from the study if indicated as HIV positive or Hepatitis C positive. Nonetheless, all samples were treated as possibly containing bloodborne pathogens. The inactivated synovial fluid samples were then mechanically vortexed and further diluted one part synovial fluid with two parts purified deionized (DI) water, and then diluted with an additional 10% by volume of pure ethyl alcohol. The ethyl alcohol was added in an effort to reduce viscosity and as a preservative. The solution was then mechanically vortexed and ultrasonicated prior to filtration. The solution was then filtered through a 20- μm filter to remove gross debris and large particulates. All samples were stored in a refrigerator prior to analysis.

In addition to the synovial fluid samples, wear debris particles were generated and analyzed as an experimental control. Pristine biomedical grade cobalt-chromium alloy stock was used for all control experiments, with an alloy

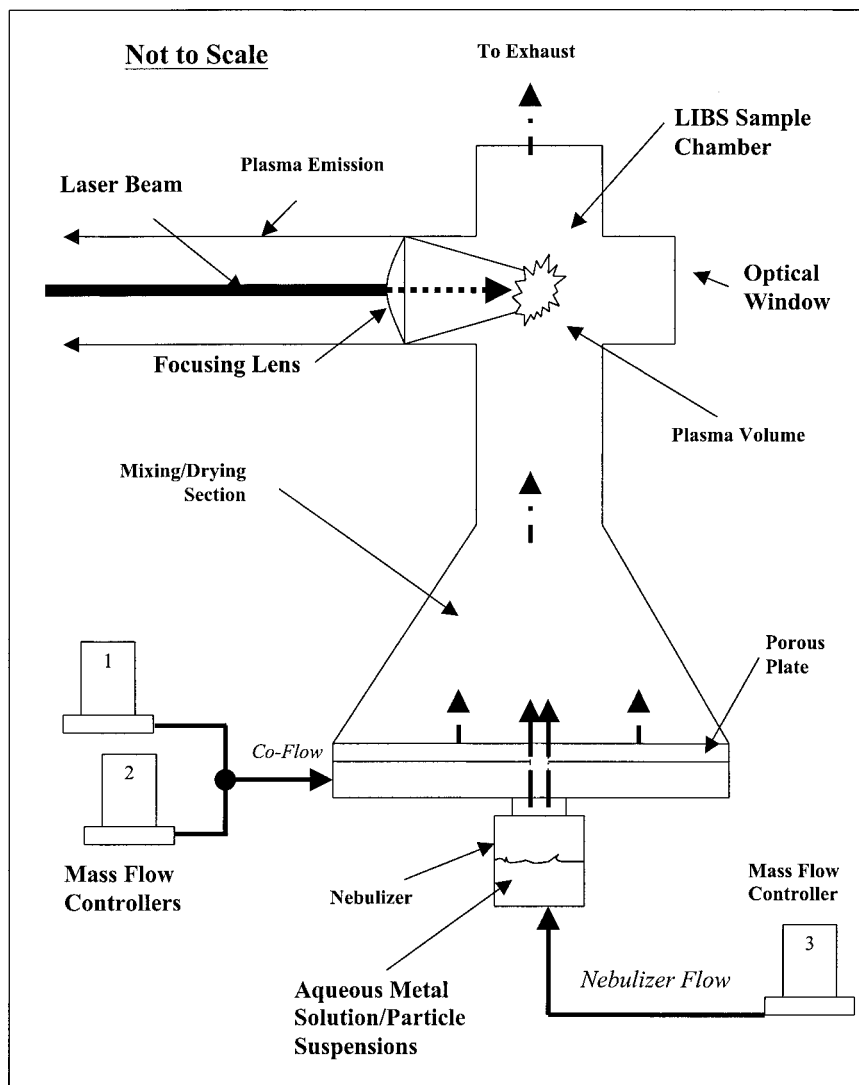


FIG. 1. Schematic of the LIBS apparatus.

composition of 62% cobalt (by weight), 26–30% chromium, 5–7% molybdenum, 1% maximum manganese, 1% maximum nickel, 1% maximum silicon, and 0.75% maximum iron. The bulk cobalt–chromium alloy density was 8.3 g/cm³. The alloy sample was manually abraded for approximately 20 min using 100-grit silicon oxide sandpaper. The accumulated wear debris was rinsed into a test tube using ultra-purified DI water, thereby creating a suspension of wear particles of a known alloy type. The particle suspension was divided into two equal volumes. One sample volume was diluted by 10% with bleach, and the second sample volume was diluted by 10% with DI water to maintain a similar particle concentration. Both samples were mechanically vortexed and stored under refrigeration for a period of 5 weeks, equal to the maximum period for which the processed synovial fluid samples were stored. This procedure was done to determine the potential effects, if any, of the added bleach on wear debris particles. It is noted that synovial samples were diluted with bleach and inactivated prior to sample processing; hence, the final synovial fluid samples utilized in this study were approximately 3.3% bleach by volume.

Therefore, the 10% bleach sample prepared to assess any possible role of bleach represents an upper limit.

Sample Analysis. The synovial fluid samples were measured using the LIBS system as follows. Processed wear particle suspensions, either synovial fluid samples or the control alloy particle suspensions, were nebulized into a co-flow air stream. The nebulized droplets subsequently dried in the co-flow stream, thereby introducing the wear particles into an aerosol stream. The particles were subsequently transported to the sampling chamber by the co-flow air stream, where the particles were enveloped by the laser-induced plasma. The aerosol stream was subsequently exhausted after leaving the sampling chamber.

EXPERIMENTAL RESULTS

LIBS Optimization and Calibration. A significant aspect of this work was the optimization of the LIBS technique for the specific application of cobalt–chromium wear particles analysis. LIBS system parameters include the laser pulse energy, temporal delay and integration

time of the CCD detection gate, and the use of either air or nitrogen for the co-flow gas stream. Laser pulse energy is an important factor in generation of a laser-induced plasma and in the subsequent analyte atomic emission signal. The threshold power required for laser-induced breakdown in ambient air is typically less than 100 mJ per pulse for a Q-switched, fundamental Nd:YAG laser wavelength. Recent work has demonstrated that additional laser pulse energy beyond the breakdown threshold functions to increase the stability (i.e., precision) of the plasma for single-shot measurements as performed in the current work.²⁰

In view of the above comments, a laser pulse energy of 330 mJ was used for all measurements. This laser pulse energy was sufficient to induce breakdown with each laser pulse, independent of aerosol loading. The intensity of the plasma emission is a strong function of time, which is a result of the time-dependent plasma temperature. For a nominal 300-mJ pulse energy, the plasma temperature is approximately 11 700, 9700, and 9000 K at delay times of 15, 25, and 100 μ s, respectively, as measured using a series of chromium emission lines.²¹ In general, the plasma emission is dominated by continuum emission (recombination and Bremsstrahlung) at relatively short delay times with respect to the incident pulse. As time increases, atoms relax electronically, resulting in additional atomic emission. An optimal temporal window for detection should maximize the atomic emission-to-continuum emission ratio. Detector gating was used to explore this behavior, with the goal of optimizing the atomic emission signal for the *simultaneous* detection of cobalt and chromium. Finally, the optimal carrier gas (nitrogen or air) was determined for the two targeted elements. In general, the gas matrix does not significantly influence plasma temperature or electron density as shown by Yalcin et al.;²² however, the atomic emission of certain analyte species may be influenced by the presence of oxygen.²¹

To simultaneously analyze cobalt and chromium atomic emission lines, specific lines were chosen that did not interfere with one another, but that were available in the approximately 35-nm spectral window realized by the grating dispersion and CCD array. The optimal lines for analysis were the chromium (I) lines at 359.35 and 360.53 nm and the cobalt (I) lines at 340.51 and 345.35 nm. The optimal LIBS parameters for detection were a temporal delay of 40 μ s with respect to the incident laser pulse and an integration time of 20 μ s. The optimal gas matrix was air, which provided an approximately factor of 3 increase in emission signal-to-noise ratio for chromium, and an approximately 50% increase in signal-to-noise for cobalt, as compared to the pure nitrogen matrix. Representative LIBS spectra for pure chromium and cobalt standards are presented in Fig. 2, corresponding to these optimal experimental conditions. The data correspond to metal concentrations of 1700 μ g/m³, or about 1.5 parts per million on a mass basis.

Once the optimal experimental parameters were determined, the standard aqueous solutions were used to produce a set of calibration curves for both pure chromium and pure cobalt solutions. The actual analyte mass concentration in the LIBS sample chamber was calculated using the predetermined nebulizer mass flow rate (0.09

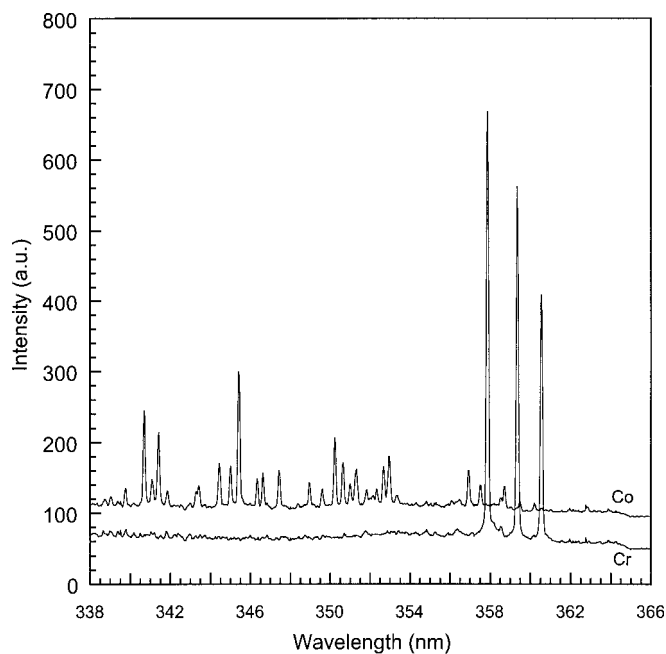


FIG. 2. LIBS spectra of chromium and cobalt sample calibration streams at a concentration of 1700 μ g/m³. Both spectra have the same scale and have been shifted vertically for clarity.

mL/min), the total gas flow rate, and the mass concentration of the analyte in the aqueous calibration solution. Calibration curves were prepared for analyte concentrations in the sample chamber ranging from 0 to 8000 μ g/m³, which corresponds to an upper limit of about 7 parts per million on a mass basis. All calibration curves were highly linear over the chromium and cobalt concentration ranges, with linear regression coefficients (R) greater than 0.99.

An additional set of experiments was performed to verify the independence of the chromium and cobalt atomic emission signals for mixtures of the two elements. Because the goal of the present work is to quantify the mass composition of individual retrieved wear particles, it is necessary to demonstrate the independence of LIBS-based analysis specifically for cobalt and chromium. In general, analyte independence is assumed for LIBS-based analysis of gaseous samples, and it was previously reported that the quantitative analysis of chromium particles was not affected by the addition of a 20-fold increase in calcium particles.¹⁷ For the present study, known concentrations of cobalt and chromium were mixed at ratios of 1-to-1, 1-to-2, and 2-to-1, corresponding to concentrations within the linear calibration ranges discussed above. The solutions were analyzed with the LIBS system, and the chromium-to-cobalt ratios were calculated based on the analyte emission signals and the respective calibration curves. The measured LIBS-based chromium-to-cobalt concentration ratios are plotted in Fig. 3 as a function of the prepared chromium-to-cobalt mixture concentrations. The slope is near unity (0.95) and the regression coefficient is 0.999, demonstrating the independence of the cobalt and chromium atomic emission signals under the present experimental conditions.

Analysis of Control Wear Particles. As discussed above, wear particles were generated from pristine ortho-

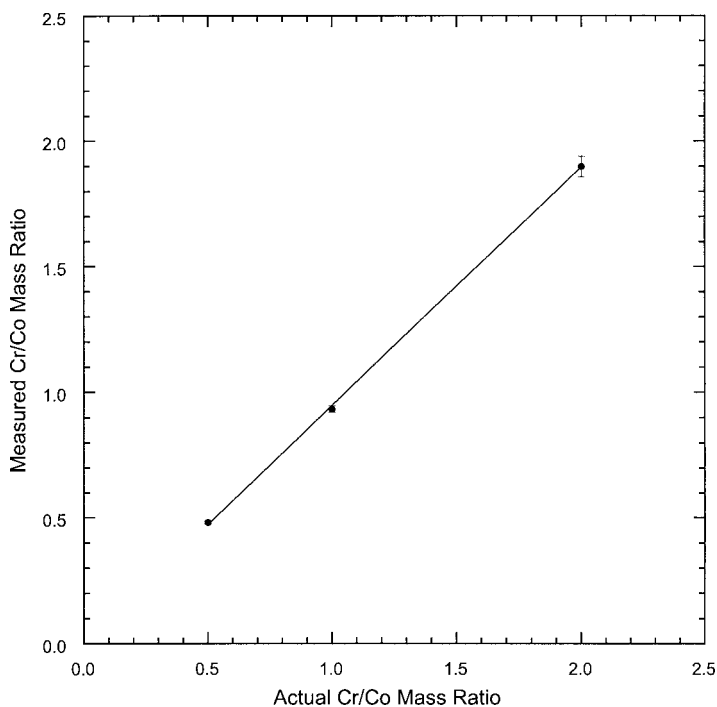


FIG. 3. LIBS-based chromium-to-cobalt mass ratios as a function of chromium-to-cobalt calibration mixture concentrations.

paedic alloys as control particles. These particles were analyzed to assess the quantitative analysis of well-defined alloy particles using the LIBS technique and to investigate possible effects of the bleach on the cobalt-chromium particles. Pure deionized water was first nebulized through the LIBS system to determine the intensity ratios of the plasma emission from the region corresponding to the targeted analyte emission lines to adjacent, featureless continuum regions. These baseline peak-to-base values were then used to define a suitable threshold value for the conditional analysis of each LIBS spectrum. The threshold was used for the identification of spectra corresponding to the presence of cobalt-chromium wear particles in a particular laser-induced plasma. The threshold was set using a 75% increase above the nominal peak-to-base values as determined for the DI water only. As discussed below, the threshold value was set to detect particles at the shot-noise limit, which also leads to the collection of “false” hits, namely extreme spectral noise fluctuations. Such spectra were subsequently rejected with the filtering algorithm. The 345.45 and 357.87 nm emission lines were used for the detection of cobalt and chromium, respectively.

The control particle suspensions were diluted with DI water by an additional factor of 1-to-3 prior to analysis. The additional dilution was performed to reduce the resulting aerosol concentration of wear particles, thereby reducing the average particle sampling rate (i.e., hit rate) to approximately 1 to 2% and reducing the possibility of multiple particle sampling (i.e., two particles in the same plasma volume). For the DI water suspensions and the bleach-treated suspensions, eight to ten 1000-shot laser sequences were performed and all spectra corresponding to either cobalt or chromium particle hits were saved for subsequent analysis. Typically, the number of cobalt-triggered

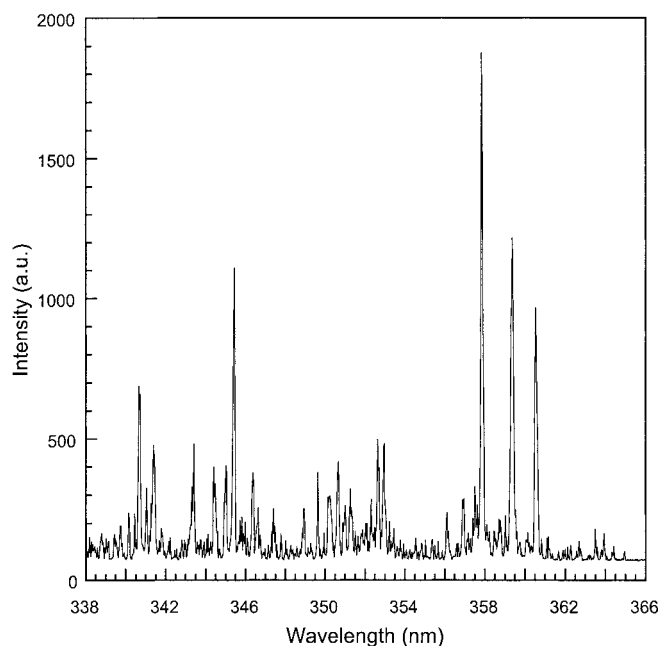


FIG. 4. Single shot LIBS spectrum corresponding to an individual cobalt-chromium wear particle.

gered particle hits was about 1/3 less than the number of chromium-triggered particle hits, which reflects the greater than four-fold increase in the peak-to-base of the chromium emission peak as compared to the cobalt emission peak. All recorded spectra were merged into a common spectral data set, and duplicate spectra were subsequently removed.

Figure 4 presents a single-shot LIBS spectrum corresponding to one of the cobalt-chromium particles recorded from the DI water suspension. As demonstrated in the figure, a single-shot spectrum can be very noisy, primarily due to the CCD intensifier shot-noise. The baseline continuum noise is quite substantial and essentially limits the overall particle analyte mass that can be identified and analyzed based on the ability to differentiate analyte emission peaks from the noise fluctuations of the continuum intensity. In order to reduce the effect of noise in the data analysis, all conditionally identified spectra (i.e., particle hits) were filtered using a series of sorting procedures. For each spectrum corresponding to a recorded hit, two different atomic emission lines were analyzed using the respective linear calibration curves for each element. Specifically, spectra were analyzed for chromium using the 359.35 and 360.53 nm Cr(I) emission lines and for cobalt using the 340.51 and 345.35 nm Co(I) emission lines. Each emission line and calibration curve yielded an equivalent mass concentration ($\mu\text{g}/\text{m}^3$), which was subsequently used to calculate the analyte mass as discussed below. Spectra were retained for single-shot analysis only if the chromium concentration calculated for the two different chromium lines agreed within a factor of two *and* the cobalt concentration calculated for the two cobalt emission lines agreed within a factor of two. This algorithm was developed earlier and was found to be a useful approach to rejecting spectra characterized by high noise on any of the relevant emission lines or atypical spectral line pairs.¹⁷ Rejection rates of

single-shot spectra ranged from 20 to 80% in the present study. It is difficult to categorize the rejected spectra as representative of actual particle hits below the detection limit or as stemming from shot noise. A careful analysis of data collection rates for various threshold values and particle stream conditions would further elucidate this issue but is beyond the scope of the present study. Detection limits are determined by the analyte signal-to-noise ratio of a single spectrum; hence, particle sizes approaching the detection limit are more difficult to measure and caution must be exercised when making inferences about the size distribution near the lower size limit. The most direct measure of the particle detection limit may be inferred from the typically sharp cutoff of measured particle size histograms (~200 nm in Fig. 7).

Once the spectra were filtered, the equivalent mass concentrations, as based on the respective analyte atomic emission lines and the mass calibration curves, were used to determine the quantitative mass composition of each recorded wear particle. For each atomic emission line, the absolute analyte mass is obtained from the product of the equivalent mass concentration ($\mu\text{g}/\text{m}^3$) and the laser-induced plasma volume V_p .¹⁷ Hence the equivalent mass concentration x physically represents the actual analyte mass in the effective plasma volume through the relation

$$x = (\text{analyte mass})/V_p \quad (1)$$

The current LIBS system was previously calibrated for the plasma volume for similar experimental parameters, yielding an effective volume of $2.5 \times 10^{-4} \text{ cm}^3$,¹⁷ which was used for the current study.

Using this approach, the absolute chromium mass was then calculated from the average values as based on each chromium emission line, and the absolute cobalt mass was calculated from the average values based on the two cobalt emission lines. These values were used to calculate the chromium-to-cobalt mass ratio for each individual wear particle analyzed, as well as the equivalent spherical particle diameter. Specifically, the particle size was calculated based on the total particle analyte mass (defined as the average cobalt mass plus the average chromium mass) and the overall bulk density of cobalt–chromium alloy (8.3 g/cm³). This yields the relationship

$$D = \left[\frac{6(\text{mass}_{\text{chromium}} + \text{mass}_{\text{cobalt}})}{\pi\rho} \right]^{1/3} \quad (2)$$

where it is noted that this expression neglects the mass contribution of the other constituent elements present in the cobalt–chromium alloy. This approximation will change the equivalent spherical diameters by less than 5% due to the cube-root dependence.

Using the above analysis, it is useful to explore the variation in the measured cobalt-to-chromium ratios for single particles. Figure 5 presents a histogram of the distribution of the chromium-to-cobalt mass ratios for the control wear particles, namely, the pure water particle suspension. The Cr/Co mass ratios range from 0.1 to 2.8, with a mean value of 0.66 and a standard deviation of 0.41. Using Eq. 2, the equivalent spherical diameter was calculated for each corresponding wear particle. The calculated diameters ranged from 230 to 720 nm, with a mean particle diameter of 416 nm and a standard deviation of 103 nm.

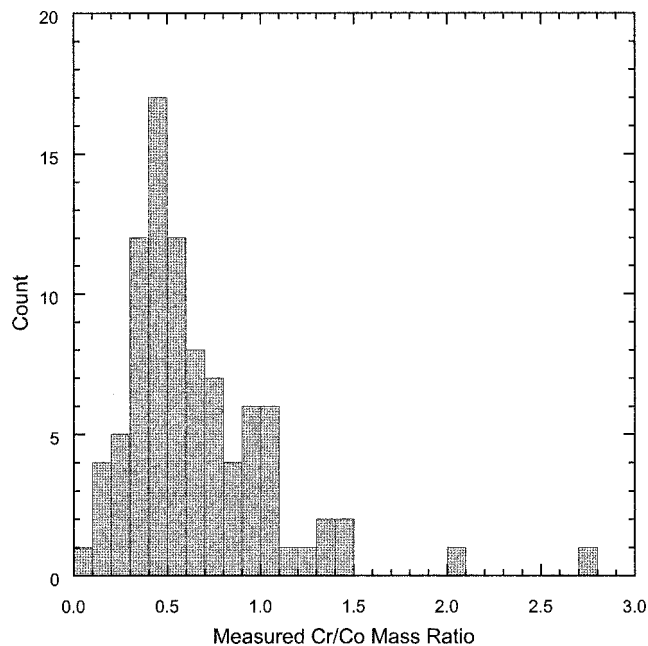


FIG. 5. Histogram of the measured chromium-to-cobalt mass ratio for the generated control cobalt–chromium wear particle suspension.

It is noted that the mean diameter of 416 nm corresponds to an absolute chromium mass of about 140 fg and an absolute cobalt mass of 190 fg, demonstrating the excellent analyte sensitivity of the LIBS technique for single particle analysis. The wear particles corresponding to the bleach suspension were analyzed in an identical manner. The average chromium-to-cobalt mass ratio for the bleach suspension was equal to 0.84 with a standard deviation of 0.68. The calculated equivalent spherical diameters ranged from 270 to 840 nm, with a mean particle diameter of 426 nm and a standard deviation of 101 nm. Using a student's t-test, there was no statistical difference between the measured particle distributions of the water and bleach suspensions for a 95% confidence interval. Accordingly, it is concluded that the 10% bleach solutions had no impact on the measured wear particle distributions (i.e., Cr/Co mass ratio and particle size) as compared to the DI water control particle distributions.

For comparison with the retrieved orthopaedic wear particles, as discussed below, it is useful to examine any size dependency of the measured chromium-to-cobalt mass ratios for the control wear particles. Figure 6 shows the variation of the chromium-to-cobalt mass ratio as a function of the equivalent spherical size for each recorded particle. Both the water and the bleach particle suspension data are presented in the figure. A linear curve fit to each of the data sets resulted in a first-degree equation with a slope of 0.0006 for the bleach suspension data and a slope of 0.0008 for the water suspension data, with both approaching a limiting value of zero slope, indicative of no size dependency. Overall, the Fig. 6 data reveal that there is no size dependency for the LIBS-based chromium-to-cobalt mass ratios for the generated control wear particles.

Because no effects on the wear particle parameters were caused through deactivation with bleach, the two

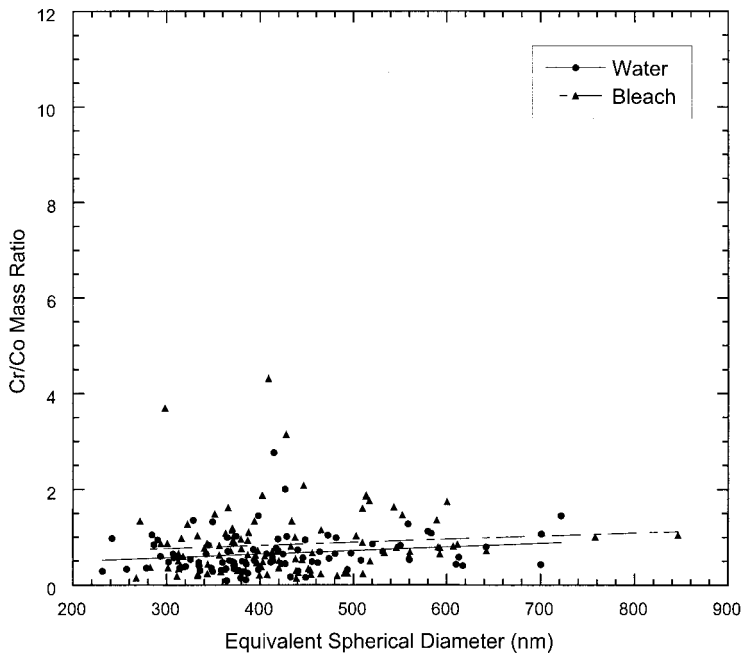


FIG. 6. Ratio of the measured chromium-to-cobalt mass ratio as a function of the measured equivalent spherical particle diameter for the generated control cobalt–chromium wear particle suspensions treated with bleach and water.

data sets presented above were combined into a single set of wear particle data representative of the cobalt–chromium wear debris generated via mechanical abrasion of the bulk alloy stock with the silicon oxide paper. To provide an independent analysis of the chromium and cobalt mass fractions within the particle suspension, additional measurements were recorded using the ICP-MS instrument. The ICP-MS measurements provide an average value of the *total* cobalt and chromium concentrations; hence, larger wear particles influence the measured concentration values more than smaller particles due to their larger masses. The mean chromium-to-cobalt mass ratio was 0.43 with a standard deviation of 0.047 as based on multiple ICP-MS measurements using different suspension concentrations. This value is in excellent agreement with the range of the Cr/Co mass ratio specified for the bulk alloy materials, namely 0.42 to 0.48. This agreement is consistent with mass conservation, in that the total mass of wear debris removed via mechanical abrasion was rinsed into the wear particle suspensions. For comparison with the ICP-MS results, the mean Cr/Co mass ratio was calculated based on the total set of LIBS data by weighting each measured particle ratio by the respective total particle mass. The LIBS-based mean Cr/Co mass ratio was 0.7, as based on the total of 195 individual wear particle measurements. The LIBS-based Cr/Co mass ratio is about 60% greater than the mass ratio specified for the bulk alloy and verified by the ICP-MS measurements for the particle suspension. It is noted, however, that the LIBS result is based on the analysis of individual wear particles between a size range of 230 and 850 nm, while the ICP-MS data is based on the analysis of *all* cobalt and chromium species within the wear debris suspension. One possible explanation is that the wear process occurs along cobalt-rich grain boundaries, there-

by producing a bi-modal distribution of wear debris, with larger wear particles that are chromium-enriched, along with smaller (i.e., nanometer-sized) cobalt-rich debris released directly along the fracture boundaries. The smaller size mode, consisting of cobalt-rich debris, would be below the LIBS detection limits for the cobalt–chromium particles (~200 nm) for the present study, but still measured adequately with the highly sensitive ICP-MS technique. Such a mechanism would explain the difference in the LIBS-based and ICP-MS results. Additional discussion regarding cobalt depletion is presented below following the presentation of the orthopaedic wear debris data.

Analysis of Retrieved Orthopaedic Wear Particles.

Four synovial fluid samples were analyzed in the present study. Two samples were collected from patients undergoing primary knee arthroplasty. These two samples served as control samples, as the joints contained no orthopaedic implant materials at the time at which the samples were collected. Two additional samples were collected from patients undergoing revision surgery of total knee replacements. For both samples, the corresponding total knee replacement contained a cobalt–chromium femoral component as the articulating component and an ultrahigh molecular weight polyethylene insert as the load-bearing counter surface. The polyethylene inserts were supported on titanium tibial trays fixed to the tibia bone without the use of PMMA bone cement.

For LIBS-based analysis as described above, approximately 5 mL of the processed synovial fluid samples was placed in the nebulizer reservoir. It was found that a significant amount of foam was immediately formed within the nebulizer upon introduction of the nebulizer gas flow. Once the nebulizer chamber was filled with foam, it effectively blocked or scrubbed the nebulizer output, precluding the introduction of any wear particles into the aerosol gas sample stream. Synovial fluid functions as a viscous lubricant for human joints and is characterized by a high surface tension resulting in the foaming action upon pneumatic agitation within the nebulizer. Various dilutions of the processed synovial fluid samples with deionized water were explored, along with the use of a commercial de-foamer; however, no combination was successful in eliminating the formation of foam for any reasonable concentration of synovial fluid. The introduction of synovial fluid to the LIBS sample stream remained intermittent and was highly dependent on the erratic and non-reproducible foam formation processes. Future work will focus on the introduction of synovial fluid to the LIBS sample chamber, possibly using non-recirculating nebulizers such as concentric-flow models typically used for ICP instruments. A limitation of such models is the relatively large sample introduction rate, typically on the order of 1 to 2 mL/min, which would present problems due to the rather limited volumes of synovial fluid available.

Sample introduction problems notwithstanding, LIBS-based analysis was achieved and a number of cobalt–chromium wear particle hits were recorded for the first revision surgery synovial fluid sample. The same data filtering algorithm discussed above was applied to all recorded spectral data, yielding a final spectral data set corresponding to 65 individual wear particles. The spectra

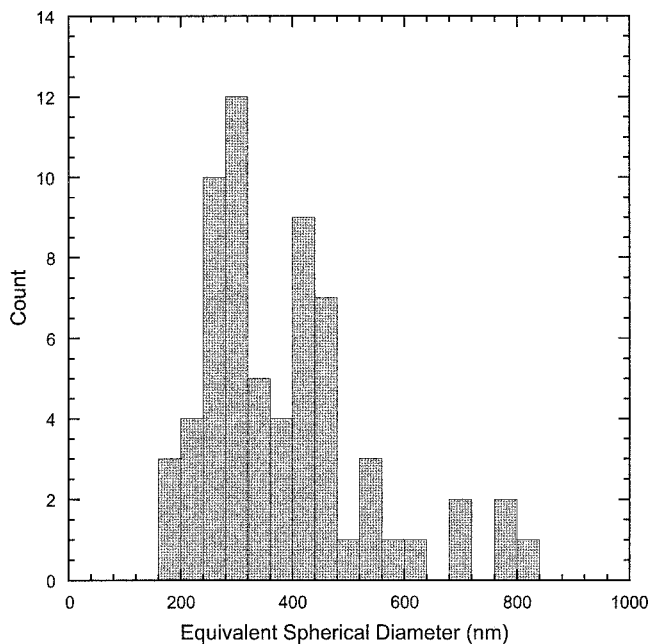


FIG. 7. Histogram of the calculated equivalent spherical particle diameter measured for the *in vivo* generated wear particles.

from all identified cobalt–chromium wear particle hits were analyzed using both of the calibrated chromium and cobalt atomic emission lines. The absolute chromium and cobalt masses were then calculated for each particle hit, along with the chromium-to-cobalt mass ratio and the equivalent spherical particle diameter using Eq. 2. Figure 7 shows a size histogram of the measured cobalt–chromium wear particles for the first revision surgery fluid sample. The mean size of the measured wear particle size distribution is 385 nm with a standard deviation equal to 147 nm. The minimum and maximum recorded diameters were 185 and 800 nm, respectively. For all the single-particle data, the individual chromium-to-cobalt mass ratios are plotted as a function of equivalent spherical diameter in Fig. 8. The plot clearly shows a significant size dependency of the chromium-to-cobalt mass ratio of the wear debris particles. Recall that the bulk composition of the alloy exhibits a chromium-to-cobalt ratio of approximately 0.44, while the measured Cr/Co mass ratios range from 0.1 to 11 in Fig. 8. Accordingly, the wear debris particles exhibit a significant amount of cobalt depletion with respect to the bulk alloy composition. Although some cobalt depletion was observed with the mechanically abraded control particles as shown in Fig. 6, comparison between the two data sets reveals a significant size-dependency of the Cr/Co ratio for the retrieved *in vivo* generated orthopaedic wear particles as compared to the control wear particles. Clearly, the size-dependent cobalt depletion is unique to the *in vivo* generated wear debris.

As with the control wear particles, ICP-MS measurements were made of the retrieved wear particles suspensions to provide an average value of the total cobalt and chromium concentrations. The mean chromium-to-cobalt mass ratio was 1.3 with a standard deviation of 0.06 as based on multiple ICP-MS measurements using different suspension concentrations. For comparison with the ICP-

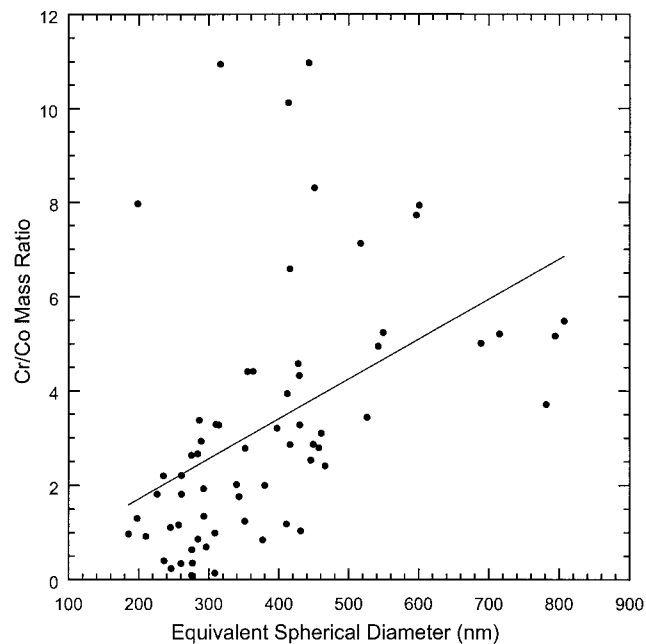


FIG. 8. Ratio of the measured chromium-to-cobalt mass ratio as a function of the measured equivalent spherical particle diameter for the *in vivo* generated wear particles.

MS results, the mean Cr/Co mass ratio was calculated based on the total set of LIBS data by weighting each measured particle ratio by the respective total particle mass. The LIBS-based mean Cr/Co mass ratio was 3.5, as calculated using a total of 65 individual wear particle measurements. Similar to the trend observed above for the control particles, the LIBS-based Cr/Co mass ratio is about a factor of three greater than the mass ratio as measured using ICP-MS. As noted above, the ICP-MS result is based on the analysis of *all* cobalt and chromium atoms within the wear debris suspension, while the LIBS-based analysis is based solely on the recorded particle hits with particles sizes in the range from about 200 to 800 nm. These data suggest that there is additional cobalt, either dissolved or present as nanometer-sized particulates, present in the processed synovial fluid samples. While the LIBS and ICP-MS techniques are characterized by different detection limits for the current implementation, both methods yielded significant depletions in the recorded cobalt mass fractions, which are reflected in the three-fold increase in the chromium-to-cobalt mass ratio with ICP-MS analysis and a six-fold increase in the mass ratio for LIBS analysis of wear particles, as compared to the pristine alloy ratio.

Limited success was achieved in nebulizing the second synovial fluid sample corresponding to a revision surgery. Only several spectra were recorded corresponding to cobalt–chromium particle hits, which after application of the filtering algorithm yielded a single wear particle hit. Analysis yielded an equivalent spherical diameter of 740 nm with a corresponding chromium-to-cobalt mass ratio of 5.3. This data point is in excellent agreement with the Fig. 8 data corresponding the first set of *in vivo* generated wear particle data, corroborating the cobalt depletion with a second implanted joint.

Finally, the control synovial fluid samples collected from patients undergoing primary knee arthroplasty were

analyzed. The joints from which the synovial samples were collected contained no implant materials; hence, these samples represent control samples and enable assessment of potential particle contamination and false particle hits. It is noted that the LIBS analysis of the four synovial fluid samples was conducted using a blind trial, in that the present investigators did not know which samples were from control or implanted joints. During data collection and analysis, no cobalt–chromium particle hits were recorded for either control sample for approximately 25 000 laser shots. However, approximately six hits were recorded as triggered on the 308.25 nm aluminum atomic emission peak. The six spectra were not fully processed for quantitative analysis of aluminum, but are consistent with the detection of submicrometer-sized contaminant aluminum particles. These contaminant particles are suspected to originate from the aluminum base plate and mounting screws of the nebulizer holder, which form part of the aerosol stream generation system and are periodically removed for cleaning.

RESULTS AND DISCUSSION

In this study the LIBS technique has been evaluated as a means of providing quantitative elemental mass and size analysis for single submicrometer-sized (as low as 185 nm) cobalt–chromium wear particles. A key advantage in using the LIBS technique for the simultaneous analysis of cobalt and chromium is the availability of multiple atomic emission lines for each element within an accessible spectral window. Multiple emission lines enabled the implementation of a spectral data filtering process, whereby the ratio of the calculated analyte signals from two separate emission lines was used to reject excessively noisy spectra, atypical spectra, or spectra corresponding to extreme shot noise. Overall, the current experimental parameters are well suited for the analysis of cobalt–chromium wear particles.

The ability of the LIBS technique to provide quantitative measurements of the size and composition of cobalt–chromium alloys was investigated by analyzing wear particles generated from pristine alloy samples as well as *in vivo* generated wear particles as collected from synovial fluid samples of implanted joints. The LIBS technique was successful in providing single-particle measurements of the absolute chromium and cobalt mass, which enabled calculation of chromium-to-cobalt mass ratios and the equivalent spherical diameter on a particle-to-particle basis. Absolute cobalt and chromium mass measurements were made as low as 40 and 20 fg, respectively, corresponding to a particle diameter of approximately 200 nm. It is noted that the upper limit for complete dissociation of single particles should be considered in the current application of quantitative analysis. An upper size limit of 10 μm is frequently cited in the LIBS literature, although recent work by the authors suggests a value on the order of several micrometers. Nonetheless, the submicrometer-sized particles analyzed in this study are well within the expected limits for complete vaporization.

From a practical point of view, all synovial fluid samples were inactivated in 10% bleach to reduce risks of infection by bloodborne pathogens. Therefore, the poten-

tial effect of bleach on control cobalt–chromium particles was also investigated. The particle size distributions and chromium-to-cobalt mass ratios were calculated and compared for both bleach suspensions and control water suspensions. No statistical differences were recorded between the two particle suspensions, supporting the conclusion that bleach had no particular effect on any of the wear particles under the experimental conditions, thereby making bleach inactivation a viable approach for future experiments.

The primary goal of this work was the implementation and use of laser-induced breakdown spectroscopy for the quantitative analysis of metallic wear debris generated within artificial joints; hence, as a pilot study, only a few synovial fluid samples were examined. A significant amount of knowledge was gained with regard to the introduction of synovial fluid samples into the LIBS sample chamber. The current use of a pneumatic-type medical nebulizer was not optimal for the nebulization of synovial fluid samples. Specifically, the agitation and recirculating nature of the fluid sample reservoir in the nebulizer combined with the high surface tension of the synovial fluid solutions resulted in an unacceptable amount of foam formation within the nebulizer. The foam functioned to scrub the nebulized droplets, thereby eliminating the steady introduction of wear debris into the co-flow air stream for subsequent transport to the LIBS sample beam. Future research will focus on more reliable means of introducing synovial fluid samples, including the use of alternative nebulizer configurations.

Based on the current LIBS analysis, the size of the *in vivo* generated wear debris ranged from approximately 200 to 800 nm, with a mean diameter of 385 nm. This data compares very favorably with reported wear debris data based on microscopy studies of retrieved cobalt–chromium wear particles. Margevicius et al. report a mode of the measured distribution function that ranged from 580 nm (the lower limit of detection) to 790 nm based on visible light microscopy,⁹ and Maloney et al. report a similar value of 700 nm based on scanning electron microscopy.¹⁰ It is noted that visible light microscopy is biased toward the largest submicrometer-sized particles due to the optical resolution of the technique. A scanning electron microscopy study of retrieved cobalt–chromium wear debris revealed a modal diameter between 250 and 500 nm, with approximately half of the analyzed particles less than 1 micrometer in size.¹

For the generated control wear particle suspensions, single-particle chromium-to-cobalt mass ratios exhibited a slight increase with respect to the alloy composition (approximately 0.7 compared to 0.44 for the bulk alloy), consistent with an overall depletion of cobalt. The depletion of cobalt was much more pronounced in the data set corresponding to the *in vivo* generated wear particles. In addition, the depletion of cobalt in the *in vivo* wear particles exhibited a strong correlation with size, with the larger particles characterized by a more significant depletion in cobalt over an overall size range between 250 and 800 nm. The size dependent nature of the cobalt depletion suggests that this phenomenon is not associated with simple cobalt dissolution of wear debris within the synovial fluid. Such a dissolution process would be dependent on surface area, and would therefore be expected to exhibit

an inverse relationship of cobalt depletion with particle size. The opposite trend was observed with the cobalt–chromium wear particles. Changes in the chromium/cobalt mass ratios have been reported previously for orthopaedic wear debris, with a number of studies reporting the bulk Cr/Co mass ratio in retrieved tissue samples collected from around the implanted joint.^{1,23,24} The reported chromium-to-cobalt mass ratios in these studies ranged as high as nine, with all of the cited Cr/Co ratio values exceeding two. More significant to the present study, electron microprobe elemental analysis was used to analyze retrieved cobalt–chromium wear debris. The results showed that the cobalt mass fraction was reduced to near zero values.²⁵ Such a depletion of cobalt observed in the *in vivo* generated wear debris samples may provide insight into the tribological wear mechanisms. For example, are wear particles produced by failure along cobalt-rich grain boundaries, thereby generating locally chromium-rich wear particles? A recent study of cobalt–chromium porous coatings on orthopaedic implants revealed that corrosion behavior consists of a generalized dissolution of the cobalt-rich matrix, with preferential attack of the grain boundaries surrounding the carbides.²⁶ Overall, the information rich data produced by single-particle LIBS-based analysis will hopefully provide bioengineers with additional knowledge to better understand the complicated processes associated with *in vivo* wear of metallic components.

ACKNOWLEDGMENTS

The authors would like to acknowledge the generous assistance and guidance of Liza Eschbach for the processing of the synovial fluid samples, Janina Gutierrez of the UF Department of Chemistry for her kind assistance with ICP-MS measurements, Butch Landsiedel for assistance with the medical records and sample cataloging, and Donna Wheeler, Peter Gearen, and Scott Myers for facilitating the collection of samples. The authors would also like to acknowledge funding provided for this pilot project by the UF Biomedical Engineering Program through a Whitaker Foundation Special Opportunity Award.

- ner, R. Schenk, and M. Semlitsch, *Clin. Orthop. Relat. Res.* **329**, S160 (1996).
2. M. Schmidt, H. Weber, and R. Schon, *Clin. Orthop. Relat. Res.* **329**, S35 (1996).
3. J. J. Jacobs, J. L. Gilbert, and R. M. Urban, *J. Bone Joint Surg.* **80**, 268 (1998).
4. V. J. Tomazic-Jezic, K. Merritt, and T. H. Umbreit, *J. Biomed. Mater. Res.* **55**, 523 (2001).
5. O. Gonzalez, R. L. Smith, and S. B. Goodman, *J. Biomed. Mater. Res.* **30**, 463 (1996).
6. W. J. Maloney, R. L. Smith, F. Castro, and D. J. Schurman, *J. Bone Joint Surg.* **75**, 835 (1993).
7. D. W. Howie, S. D. Rogers, M. A. McGee, and D. R. Haynes, *Clin. Orthop. Relat. Res.* **329**, S217 (1996).
8. D. R. Haynes, S. D. Rogers, S. Hay, M. J. Percy, and D. W. Howie, *J. Bone Joint Surg.* **75**, 825 (1993).
9. K. J. Margevicius, T. W. Bauer, J. T. McMahon, S. A. Brown, and K. Merritt, *J. Bone Joint Surg.* **76**, 1664 (1994).
10. W. J. Maloney, R. L. Smith, T. P. Schmalzried, J. Chiba, D. Huene, and H. Rubash, *J. Bone Joint Surg.* **77**, 1301 (1995).
11. P. F. Doorn, P. A. Campbell, and H. C. Amstutz, *Clin. Orthop. Relat. Res.* **329**, S206 (1996).
12. H. Zhang, F. Y. Yueh, and J. P. Singh, *Appl. Opt.* **38**, 1459 (1999).
13. R. E. Neuhauser, U. Panne, R. Niessner, G. A. Petrucci, P. Cavalli, and N. Omenetto, *Anal. Chim. Acta* **346**, 37 (1997).
14. K. Song, Y.-I. Lee, and J. Sneddon, *Appl. Spectrosc. Rev.* **32**, 183 (1997).
15. J. Sneddon and Y.-I. Lee, *Anal. Lett.* **3**, 2143 (1999).
16. D. A. Rusak, B. C. Castle, B. W. Smith, and J. D. Winefordner, *Crit. Rev. Anal. Chem.* **27**, 257 (1997).
17. D. W. Hahn and M. M. Lunden, *Aerosol Sci. Technol.* **33**, 30 (2000).
18. J. E. Carranza, B. T. Fisher, G. D. Yoder, and D. W. Hahn, *Spectrochim. Acta, Part B* **56**, 851 (2001).
19. D. W. Hahn, J. E. Carranza, G. R. Arsenault, H. A. Johnsen, and K. R. Hencken, *Rev. Sci. Instru.* **72**, 3706 (2001).
20. J. E. Carranza and D. W. Hahn, *Spectrochim. Acta, Part B* **57**, 779 (2002).
21. R. L. Gleason and D. W. Hahn, *Spectrochim. Acta, Part B* **56**, 419 (2001).
22. S. Yalcin, D. R. Crosley, G. P. Smith, and G. W. Faris, *Haz. Waste Haz. Mater.* **13**, 51 (1996).
23. E. M. Evans, M. A. R. Freeman, A. J. Miller, and B. Vernon-Roberts, *J. Bone Joint Surg.* **56**, 626 (1974).
24. M. Semlitsch and H. G. Willert, *Microchim. Acta* **1**, 21 (1971).
25. B. F. Shahgaldi, F. W. Heatley, A. Dewar, and B. Corrin, *J. Bone Joint Surg.* **77**, 962 (1995).
26. H. E. Placko, S. A. Brown, and J. H. Payer, *J. Biomed. Mater. Res.* **39**, 292 (1998).

1. H. G. Willert, G. H. H. Buchhorn, D. Gobel, G. Koster, S. Schaff-